

Highly Selective Ruthenium Metathesis Catalysts for Ethenolysis

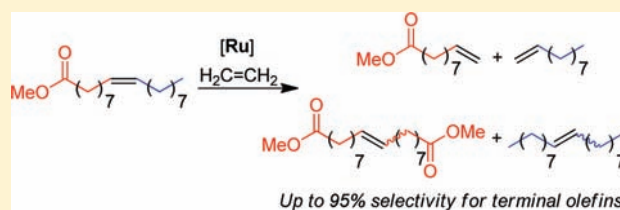
Renee M. Thomas,[†] Benjamin K. Keitz,[†] Timothy M. Champagne,[‡] and Robert H. Grubbs^{*,†}

[†]The Arnold and Mabel Beckman Laboratories of Chemical Synthesis, Division of Chemistry and Chemical Engineering, California Institute of Technology, Pasadena, California 91125, United States

[‡]Materia, Inc., 60 North San Gabriel Boulevard, Pasadena, California 91107, United States

S Supporting Information

ABSTRACT: *N*-Aryl,*N*-alkyl *N*-heterocyclic carbene (NHC) ruthenium metathesis catalysts are highly selective toward the ethenolysis of methyl oleate, giving selectivity as high as 95% for the kinetic ethenolysis products over the thermodynamic self-metathesis products. The examples described herein represent some of the most selective NHC-based ruthenium catalysts for ethenolysis reactions to date. Furthermore, many of these catalysts show unusual preference and stability toward propagation as a methyldiene species and provide good yields and turnover numbers at relatively low catalyst loading (<500 ppm). A catalyst comparison showed that ruthenium complexes bearing sterically hindered NHC substituents afforded greater selectivity and stability and exhibited longer catalyst lifetime during reactions. Comparative analysis of the catalyst preference for kinetic versus thermodynamic product formation was achieved via evaluation of their steady-state conversion in the cross-metathesis reaction of terminal olefins. These results coincided with the observed ethenolysis selectivities, in which the more selective catalysts reach a steady state characterized by lower conversion to cross-metathesis products compared to less selective catalysts, which show higher conversion to cross-metathesis products.



INTRODUCTION

Olefin metathesis is widely used in both organic and polymer synthesis and has become a standard methodology for constructing carbon–carbon double bonds.¹ Metathesis catalysts have been successfully designed for stability,² functional group tolerance,³ activity,⁴ and selectivity,⁵ enabling metathesis methodology to be broadly applied. The development of catalysts exhibiting preference for kinetically versus thermodynamically controlled product ratios continues to be a challenging area in olefin metathesis.⁶ An example of a metathesis reaction that requires kinetic selectivity is ethenolysis, the reaction of an internal olefin with ethylene to generate thermodynamically disfavored terminal olefin products. There is significant interest for selective formation of terminal olefins due to the potential conversion of fatty acids derived from renewable biomass to valuable commercial products.⁷ Such a process would enable the “green” synthesis of commercial commodities from renewable source materials such as natural seed oils and their derivatives instead of petroleum products.⁸ Natural seed oils are particularly attractive due to their built-in functionality, widespread availability, and relatively low cost. Specifically, ethenolysis of methyl oleate (MO) affords chemically desirable products with extensive applications, including use in cosmetics, detergents, soaps,⁷ and polymer additives,⁹ as well as potential applications as a renewable biofuel source.¹⁰

Most reported studies have focused on ruthenium complexes in the development of an efficient ethenolysis catalyst due to their functional group tolerance and stability to air and water, which

renders them easy to handle and does not require extensive purification of starting material.¹¹ High selectivities and yields for the ethenolysis of methyl oleate and cyclooctene have been disclosed by Schrock and co-workers using molybdenum systems.¹² Molybdenum metathesis catalysts gave up to 99% selectivity for the ethenolysis of methyl oleate in up to 95% yield, with turnover numbers (TONs) as high as 4750. Ideally, selective ethenolysis would be carried out by robust catalysts exhibiting high TONs for an efficient process. Accordingly, our research efforts are directed toward the development of ruthenium-based catalysts exhibiting these attributes for selective ethenolysis.

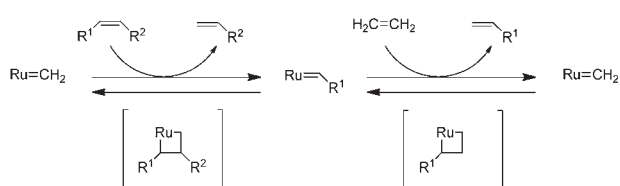
Ethenolysis reactions require catalyst stability as a propagating methyldiene species for high product selectivity and TON.^{6,13} The desirable ethenolysis catalytic cycle involves crossing an internal olefin onto the active metal complex to generate an alkylidene species, followed by reaction with ethylene to form a 1,2-metallacycle (Scheme 1). Breakdown of this metallacycle then yields the desired terminal olefin and a ruthenium methyldiene species. The methyldiene complex can react with the substrate to release a terminal olefin and afford a ruthenium alkylidene species, which can subsequently react with ethylene and repeat the cycle. Most olefin metathesis catalysts are unstable as methyldiene complexes and possibly as the corresponding unsubstituted metallacycle, and undergo rapid decomposition.¹³ This catalyst degradation significantly limits both product

Received: January 21, 2011

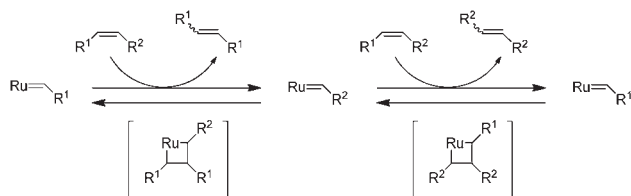
Published: April 21, 2011

Scheme 1. Cross-Metathesis Reactions during Ethenolysis

Ethenolysis Reaction



Self-Metathesis



Secondary Metathesis

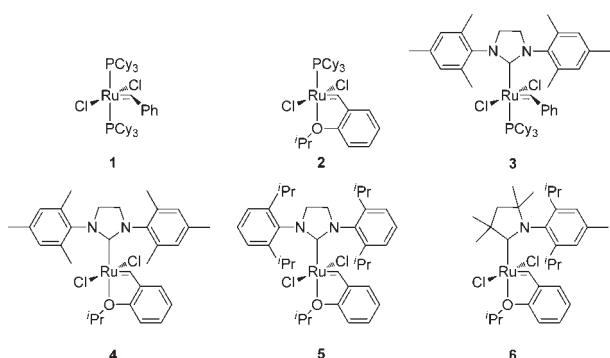
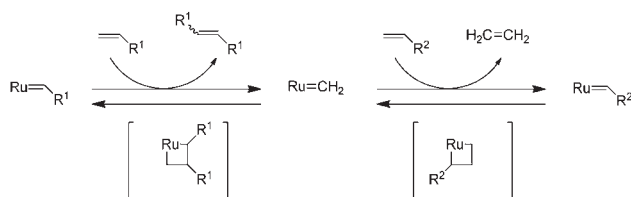
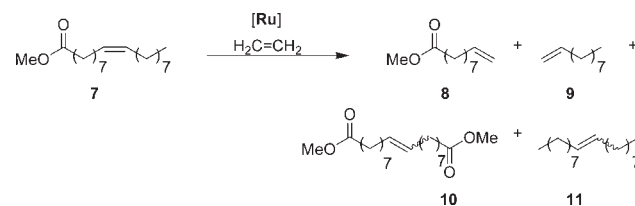


Figure 1. Example ruthenium catalysts previously studied for ethenolysis reactions.

selectivity and TON during ethenolysis reactions. Side reactions that would reduce product selectivity include self-metathesis and secondary metathesis (Scheme 1).⁶ Self-metathesis occurs when the substrate-bound catalyst reacts with another substrate molecule rather than ethylene, thereby yielding another internal olefin and ruthenium alkylidene species. Secondary metathesis involves further cross-metathesis of two desired terminal olefins to generate an internal olefin and release ethylene. Because the key steps involve propagation via a ruthenium methylidene, catalyst stability as a propagating methylidene is essential for viable ethenolysis reactions.

A variety of ruthenium metathesis catalysts have been screened for kinetic selectivity for the ethenolysis of internal olefins (Figure 1).¹⁴ Phosphine-based ruthenium catalysts (**1** and **2**, Figure 1) show high initial selectivity, where selectivity is defined as the percentage of the product mixture that is the

Scheme 2. Ethenolysis of Methyl Oleate



desired olefin products **8** and **9**, for the ethenolysis of methyl oleate (Scheme 2). However, these complexes decompose due to the instability of the propagating methylidene species, resulting in a limited catalyst lifetime. Complex **1** catalyzes the ethenolysis of methyl oleate (**7**), with 93% selectivity for ethenolysis products **8** and **9** over self-metathesis products **10** and **11**. The yield (54%) is moderate, although the TON (5400) is good. The first-generation chelate catalyst **2** improves selectivity slightly to 94%, but the yield (48%) and TON (4800) are lower.¹⁴ Catalyst inhibition by ethenolysis products is reported for the first-generation ruthenium catalysts, and instability of the methylidene undermines the use of these catalysts.^{6,7} Phoban ruthenium catalysts are reported to have some increased stability relative to first-generation catalysts, while maintaining comparable selectivities and TONs.¹⁵

NHC ruthenium catalysts are known to be very active for self-metathesis and cross-metathesis of methyl oleate with 2-butene (TON of up to 470 000).^{14,16} These complexes propagate as an alkylidene and are known to be unstable as a methylidene, leading to their inability to viably produce metathesis products requiring steps involving propagation as a methylidene. Accordingly, the selectivity of these complexes (**3–5**, Figure 1) for the production of terminal olefins **8** and **9** is poor. It has been reported that complex **3** exhibits only 44% selectivity for ethenolysis products **8** and **9** with 28% yield at a TON of 2800. Catalyst **4** was shown to display even lower selectivity at 33% and only 20% yield with a TON of 2000. However, increasing the temperature from 40 to 60 °C improved the selectivity to 47% and the yield to 32% with a TON of 3200. More sterically hindered NHC ligands also improved selectivity. Complex **5** afforded ethenolysis products **8** and **9** in 55% selectivity over **10** and **11**, with 38% yield and a TON of 3800.¹⁶ While *N*-aryl,*N*-aryl NHC-based ruthenium catalysts are generally more active and stable than first-generation catalysts, they are significantly less selective for ethenolysis due to their propensity to undergo self-metathesis reactions.

Cyclic (alkyl)(amino)carbene (CAAC) ruthenium catalysts, such as **6**, have been found to be more selective for ethenolysis products over self-metathesis products. However, improvements in selectivity, activity, and catalyst stability are still necessary for the reaction to be viable.⁶ With complex **6**, selectivities as high as 92% have been achieved at 100 ppm loading, with 56% yield and a TON of 5600. Changing the isopropyl aryl substituents to ethyl substituents improved the TON to 35 000 at 10 ppm loading, although the selectivity was reduced to 83% and the yield to 35%. These complexes are unusual in that they exhibit a higher preference for propagation as a methylidene relative to previously reported NHC-based complexes.¹⁷

Previous work in our group studying degenerate metathesis reactions has demonstrated that greater catalyst preference for a methylidene species appears to be related to selectivity for

degenerate metathesis over productive metathesis.¹⁷ Therefore, degenerate metathesis studies can be used as a means of identifying promising catalysts for ethenolysis reactions. For instance, CAAC catalysts, such as **6**, exhibit higher degenerate turnovers than **1–5**. Interestingly, unsymmetrical *N*-aryl,*N*-alkyl NHC catalysts feature even higher preference for unproductive turnovers.¹⁷ This led us to believe that these catalysts would show promising ethenolysis selectivity, with the propensity to propagate as a methylidene species providing the desired kinetic selectivity for terminal olefin products over thermodynamically favored internal olefins.

Herein, we describe the unusual stability of unsymmetrical *N*-aryl,*N*-alkyl NHC catalysts toward propagation as a methylidene species and their application as catalysts for highly selective ethenolysis. Most of the catalysts also display good thermal stability, and all are stable to air and moisture. In comparison to standard NHC and phosphine-derived ruthenium catalysts (**1–5**), these complexes exhibit longer lifetimes in cross-metathesis reactions, presumably as a result of their stability to existing as a methylidene.

RESULTS AND DISCUSSION

With the goal of improving both selectivity and TON during ethenolysis reactions, a variety of *N*-aryl,*N*-alkyl NHC complexes bearing different ligand substituents were designed and synthe-

Table 1. Catalyst Comparison for the Ethenolysis of Methyl Oleate

entry ^a	catalyst	conv (%) ^b	selectivity (%) ^c	yield (%) ^d	TON ^e
1	12	54	86	46	4620
2	13	11	77	9	845
3	15	52	86	45	4450
4	16	42	86	36	3600
5	17	59	87	51	5070
6	18	52	89	46	4604
7	19	15	95	15	1460
8	20	17	69	11	1120
9	21	40	79	31	3080

^a The reactions were run neat for 6 h at 40 °C and 150 psi of ethylene. The catalyst loading was 100 ppm. ^b Conversion = $100 - [(final\ moles\ of\ 7) \times 100 / (initial\ moles\ of\ 7)]$. ^c Selectivity = $(moles\ of\ ethenolysis\ products\ 8\ and\ 9) \times 100 / (moles\ of\ total\ products\ 8 + 9 + 10 + 11)$. ^d Yield = $(moles\ of\ ethenolysis\ products\ 8 + 9) \times 100 / (initial\ moles\ of\ 7)$. ^e TON = $yield \times [(moles\ of\ 7) / (moles\ of\ catalyst)]$.

sized (Figure 2). Complex **12** was targeted first to enhance the ethenolysis selectivity through increased steric bulk of the *N*-aryl and, primarily, the *N*-alkyl substituent. Initial screening of catalyst **12** for the ethenolysis of methyl oleate afforded promising results (Table 1, entry 1). At 150 psi of ethylene and 40 °C, 86% selectivity for ethenolysis products **8** and **9** over cross-metathesis products **10** and **11** was achieved, with 46% yield of **8** and **9** in 6 h and a TON of 4620 at a low catalyst loading of 100 ppm. The yield increased to 68% of ethenolysis products at a loading of 500 ppm, although the TON was reduced to 1370. Lowering the loading of **12** to 10 ppm gave a significantly higher TON of 8340, although the yield of **8** and **9** was only 8% after 4 h. Since good kinetic selectivity and TONs were obtained with **12**, further efforts were directed toward synthesizing new complexes to determine the effect of the NHC ligand substituents on catalyst behavior and toward identifying a catalyst with excellent kinetic selectivity (Figure 2, **12–21**). Crystal structures of complexes **12** and **15** confirmed the expected geometry and that their bond lengths are consistent with those of previously reported NHC ruthenium complexes (Figures 3 and 4).

Complexes **12–21** were all compared for catalytic activity for the ethenolysis of methyl oleate at 100 ppm catalyst loading and 150 psi of ethylene (Table 1). Complex **13** exhibited lower kinetic selectivity compared to **12** (Table 1, entry 1), with 77% selectivity for **8** and **9** over **10** and **11** (Table 1, entry 2), presumably due to the decreased sterics of the *N*-aryl substituent

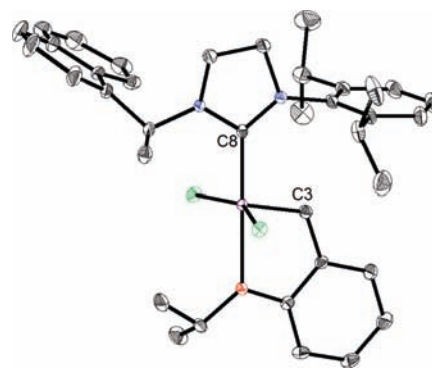


Figure 3. Crystal structure of complex **12** shown at the 50% ellipsoid probability level. Selected bond lengths: Ru–C3 = 1.83 Å, Ru–C8 = 1.98 Å, Ru–O = 2.26 Å.

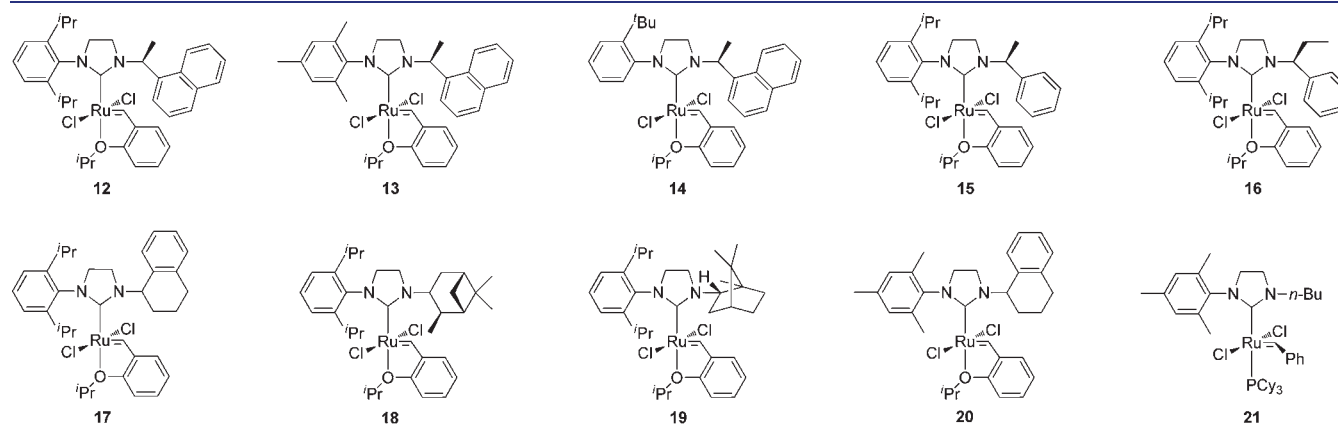


Figure 2. *N*-Aryl,*N*-alkyl NHC ruthenium complexes synthesized to selectively catalyze ethenolysis.

(mesityl in complex **13** versus 2,6-di-isopropyl phenyl in complex **12**). The TON was lower for **13** in comparison to **12** as well, likely a result of greater instability of **13** as a propagating methylenide species. Catalyst **14** was very unstable and degraded early during the reaction, affording low conversion. Since the reaction equilibrium was not reached due to the catalyst's fast decomposition, the selectivity most likely does not represent the inherent selectivity of **14** and is therefore not reported.

The kinetic selectivities of **12**, **15**, and **16** were identical (86% for **8** and **9** over **10** and **11**), suggesting that small changes in the sterics of the alkyl substituents do not have a significant impact on catalyst selectivity (Table 1, entries 1, 3, and 4). The more sterically demanding ligand substituents of **17** and **18** did slightly improve kinetic selectivity (Table 1, entries 5 and 6). High selectivities of 87% and 89% for **17** and **18**, respectively, were obtained, and both **17** and **18** displayed good TONs of 5070 and 4600, respectively. Catalyst **19** showed excellent kinetic selectivity at 95%, markedly higher than those of other reported ruthenium NHC catalysts and comparable to those of first-generation ruthenium catalysts (Table 1, entry 7).

Catalysts **20** and **21** gave lower selectivity compared to the catalysts with a di-isopropyl *N*-aryl group on the NHC, as

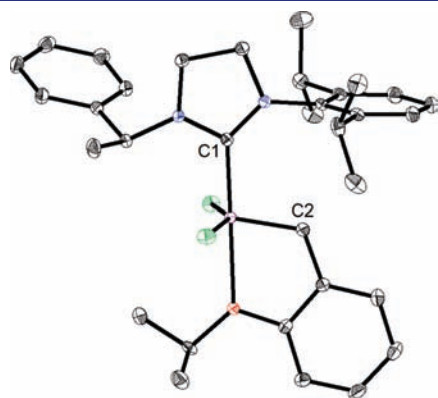


Figure 4. Crystal structure of complex **15** at the 50% ellipsoid probability level. Selected bond lengths: Ru–C2 = 1.83 Å, Ru–C1 = 1.97 Å, Ru–O = 2.28 Å.

expected from the results with **13** and **14**. The selectivities of **20** and **21** were 69% and 79%, respectively (Table 1, entries 8 and 9). The yield (40%) and TON (3080) of **21** were significantly better than those of **20** and **13**. Comparison of the various complexes screened shows a consistent trend that both *N*-aryl and *N*-alkyl groups with more sterically hindering substituents improve the desired selectivity. Di-isopropyl *N*-aryl groups enhance catalyst stability, leading to better product yields. Our next efforts were directed toward exploring catalyst loadings for the more promising catalysts for the ethenolysis of methyl oleate (Table 2).

Raising the catalyst loading to 500 ppm showed significant improvement in yield, more than doubling it in many cases, for the same given amount of time. Specifically, going from a loading of 100 ppm to 500 ppm of **19** increased the ethenolysis product yield from 15% to 46% (Table 2, entries 1 and 2). Alternatively, lowering the catalyst loading to 50 ppm decreased the yield from 15% to 5% (Table 2, entry 3). Similar results were obtained for the other catalysts upon varying catalyst loading. Complex **17**, at 500 ppm loading, generated an ethenolysis product yield of 78% (Table 2, entry 4), compared to 51% at 100 ppm (Table 2, entries 5). Analogously, **16** gave an ethenolysis yield of 72% at 500 ppm (Table 2, entry 7), compared to 36% yield at 100 ppm (Table 2, entry 8). Conversion of methyl oleate increases with higher catalyst loading, as demonstrated with **21** (Table 2, entries 10–13). Complexes **14** and **18** have markedly higher ethenolysis product yields at 500 ppm as well (Table 2, entries 14 and 15). While the selectivities remain constant at variable catalyst loading for most complexes, catalyst **14** shows increased selectivity at a 500 ppm loading compared to a 100 ppm loading (58% versus 19%). This is believed to be due to the fast degradation of **14** during the reaction. Higher loading of **14** enables the catalyst to come closer to its inherent steady state for the reaction before all of the complex has decomposed. Previous ruthenium metathesis catalyst studies have shown that having an ortho-H on the *N*-aryl ring increases the rate of catalyst decomposition.

Temperature-dependent studies were conducted using catalysts **17** and **16** to consider the effect of temperature on selectivity and TON (Table 3). Ethenolysis of methyl oleate was carried out

Table 2. Ethenolysis of Methyl Oleate Using Different Catalyst Loadings

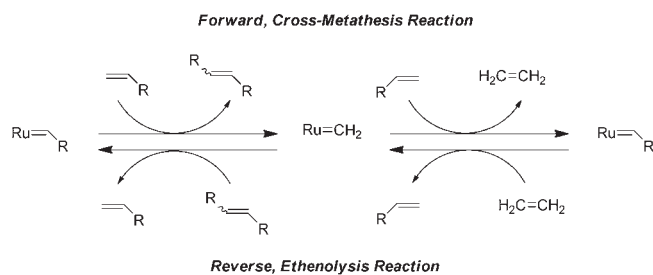
entry ^a	catalyst	cat./MO (ppm)	time (h)	conv (%) ^b	selectivity (%) ^c	yield (%) ^d	TON ^e
1	19	500	6	48	95	46	913
2	19	100	6	15	95	15	1460
3	19	50	6	5	96	5	1010
4	17	500	6	89	88	78	1570
5	17	100	6	59	87	51	5070
6	17	50	2	12	86	10	2050
7	16	500	2	83	86	72	1440
8	16	100	6	42	86	36	3600
9	16	50	6	12	87	10	2010
10	21	500	4	65	82	53	1060
11	21	100	6	40	79	31	3080
12	21	50	6	19	79	14	2880
13	21	20	2	4	80	3	1680
14	14	500	6	70	58	41	817
15	18	500	6	86	88	76	1520

^a The reactions were run neat at 40 °C and 150 psi of ethylene. ^b Conversion = $100 - [(final\ moles\ of\ 7) \times 100 / (initial\ moles\ of\ 7)]$. ^c Selectivity = $(moles\ of\ ethenolysis\ products\ 8\ and\ 9) \times 100 / (moles\ of\ total\ products\ 8 + 9 + 10 + 11)$. ^d Yield = $(moles\ of\ ethenolysis\ products\ 8 + 9) \times 100 / (initial\ moles\ of\ 7)$. ^e TON = yield $\times [(moles\ of\ 7) / (moles\ of\ catalyst)]$.

Table 3. Temperature Effects on the Ethenolysis of Methyl Oleate

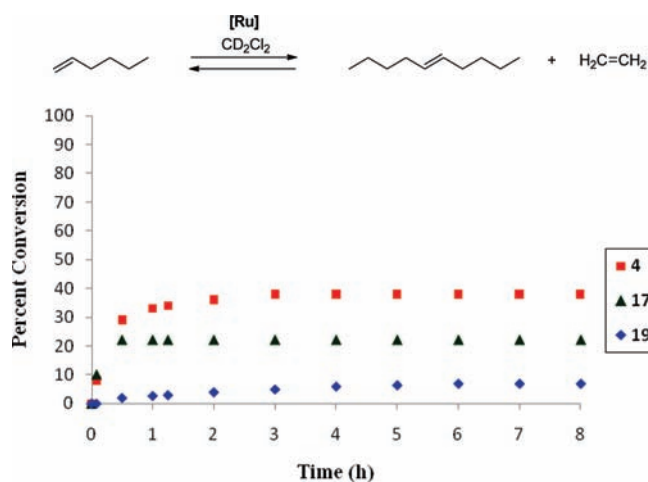
entry ^a	catalyst	temp (°C)	time (h)	conv (%) ^b	selectivity (%) ^c	yield (%) ^d	TON ^e
1	17	40	6	59	87	51	5070
2	17	50	4	67	81	55	5460
3	17	60	4	68	81	55	5470
4	16	40	6	42	86	36	3600
5	16	50	6	51	81	41	4090
6	16	60	6	47	79	37	3680

^aThe reactions were run neat at 150 psi of ethylene. The catalyst loading was 100 ppm. ^bConversion = $100 - [(final\ moles\ of\ 7) \times 100 / (initial\ moles\ of\ 7)]$. ^cSelectivity = $(moles\ of\ ethenolysis\ products\ 8\ and\ 9) \times 100 / (moles\ of\ total\ products\ 8 + 9 + 10 + 11)$. ^dYield = $(moles\ of\ ethenolysis\ products\ 8 + 9) \times 100 / (initial\ moles\ of\ 7)$. ^eTON = $yield \times [(moles\ of\ 7) / (moles\ of\ catalyst)]$.

Scheme 3. Steady State between Cross-Metathesis and Ethenolysis

at 40, 50, and 60 °C for each catalyst. The TON for both 17 and 16 increased at higher reaction temperatures, as did the product yield. A reaction temperature of 60 °C likely induces earlier catalyst decomposition and may account for the lower TON and yield for 16 at 60 °C compared to 50 °C (Table 3, entry 6). For both catalysts, the more significant increase in TON and yield occurred on going from 40 to 50 °C, indicating that further increase in temperature produces only minimal benefits and may in fact initiate catalyst decomposition. The selectivity was reduced at higher temperatures, dropping from 87% to 81% for 17 and from 86% to 81% for 16 on going from 40 to 50 °C. The reduction in selectivity between 50 and 60 °C, however, was minimal. Ethenolysis reactions were not run below 40 °C, as this would decrease both the yield and TON, undermining the catalysts' utility. Accordingly, 40 °C was determined to be the optimal temperature for the ethenolysis of methyl oleate catalyzed by these *N*-aryl,*N*-alkyl NHC complexes.

In order to evaluate catalyst propensity toward ethenolysis, we conducted a qualitative steady-state study to complement the ethenolysis results obtained. Observed selectivity in ethenolysis reactions is believed to arise from a catalyst's preference for a product distribution favoring terminal olefins, manifested in its lack of cross-metathesis reactivity. This preference can be reflected in cross-metathesis reactions as well, where if ethylene generated by cross-metathesis of two terminal olefins is trapped in the reaction vessel, the forward cross-metathesis reaction will eventually reach a steady state with ethenolysis of the internal olefin products with the generated ethylene, which affords the original terminal olefins (Scheme 3). Accordingly, relative

**Figure 5. Steady state between CM of 1-hexene and ethenolysis of 5-decene.**

preferences of different catalysts for terminal olefin versus internal olefin distributions can be determined by identifying the point at which the forward cross-metathesis reaction is equal to the reverse ethenolysis reaction. This will be observed when the conversion to internal olefin product no longer increases (the steady state has been reached) and requires that the catalyst is still active and undergoing metathesis turnovers.

For ease of measurement, homodimerization cross-metathesis was chosen as the model reaction, since the only possible product is the internal olefin dimer of the substrate. The reactions were carried out in a sealed NMR tube, preventing loss of generated ethylene, and the steady state between the forward (cross-metathesis, CM) and reverse (ethenolysis) reactions for each catalyst was measured. Although this setup does not yield absolute steady-state values, as the ethylene generated will be partitioned between the solution and the NMR tube head space, it does enable qualitative evaluation of relative steady states for catalysts screened. The degree of conversion to CM product was evaluated for catalysts 17, 19, and second-generation catalyst 4 in order to assess their relative propensities to undergo CM as compared to ethenolysis. Phosphine-based ruthenium catalyst 1 was also screened during these experiments; however, 1 decomposed prior to reaching steady state between CM and ethenolysis, and the data obtained were therefore not included. Catalysts 4, 17, and 19 did not undergo any decomposition during the course of the reaction, as confirmed by monitoring them by proton NMR spectroscopy. Catalysts 4, 17, and 19 were chosen to represent a range of selectivities for the ethenolysis of methyl oleate, with 4 showing a reported 33% selectivity, 17 showing 87% selectivity, and 19 showing 95% selectivity. In accordance with these data, catalyst 19 was predicted to reach steady state between the forward and reverse reactions at the lowest conversion to CM product (higher preference for yielding ethenolysis products), and catalyst 4 was predicted to reach steady state at the highest conversion to CM product. Catalyst 17 was expected to have a steady-state point between those of the other two complexes. Two substrates were employed for these experiments. First, the experiment was carried out using 1-hexene (Figure 5), and then a duplicate set of experiments were run with allyl chloride (Figure 6) to ascertain that the observed results were not substrate specific.

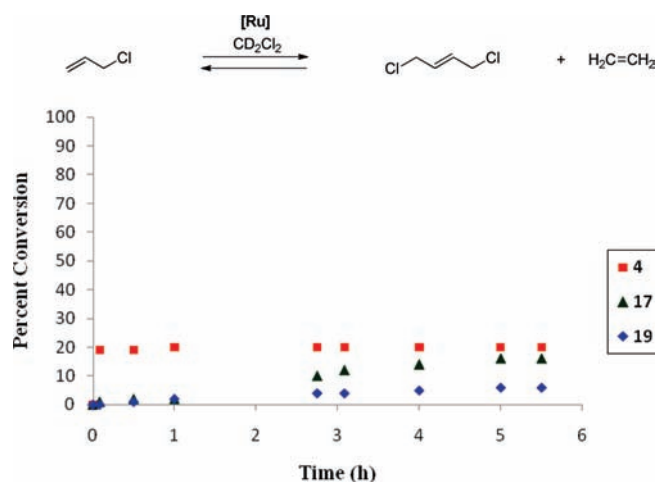


Figure 6. Steady state between CM of allyl chloride and ethenolysis of 1,4-dichloro-2-butene.

For the CM of 1-hexene and corresponding ethenolysis of 5-decene (Figure 5), the resulting relative steady-state values were as expected, with catalyst **19** showing the highest selectivity for 1-hexene (only 7% conversion to 5-decene), relative to the other catalysts, and catalyst **4** showing the lowest selectivity for 1-hexene, indicated by it producing the greatest conversion to 5-decene (38% conversion) at its steady-state point. Catalyst **17** reached steady state at 22% conversion to 1-hexene, between the values found of **19** and **4**.

When allyl chloride was used as the substrate (Figure 6), the same relative order of steady-state points was obtained for the catalysts studied. The data from both experiments corroborate the results found in the ethenolysis of methyl oleate, with **19** exhibiting the greatest preference for kinetic over thermodynamic products, and this class of *N*-aryl,*N*-alkyl catalysts showing greater preference for kinetic products than previous NHC-based ruthenium catalysts.

CONCLUSION

We have developed highly selective *N*-aryl,*N*-alkyl NHC ruthenium catalysts for ethenolysis, with **19** exhibiting the highest selectivity for an NHC-based ruthenium metathesis catalyst to date. Catalyst loadings of 500 ppm afforded good yields of the ethenolysis products **8** and **9**. The TONs were modest for most of the catalysts screened, and future studies will be directed toward improving those numbers further. These catalysts show unusual preference for generating kinetic products over thermodynamic products, which we believe to be controlled primarily through the NHC ligand sterics. Increasing the sterics of the NHC substituents enhances selectivity and, in general, improves stability as well, although a limit is reached where NHC ligands bearing extremely bulky substituents inhibit reactivity. The catalysts maintained good stability toward existing as a propagating methylidene species, making them attractive as catalysts for ethenolysis reactions. High selectivities, a challenging feature of ethenolysis reactions, were obtained for many of the complexes of this class of *N*-aryl,*N*-alkyl NHC catalysts.

EXPERIMENTAL SECTION

General Considerations. All manipulations of air- or water-sensitive compounds were carried out under dry nitrogen using a glovebox or under dry argon utilizing standard Schlenk line techniques. NMR spectra were recorded on a Varian Mercury (^1H , 300 MHz), a Varian Inova 400 (^1H , 400 MHz), or a Varian Inova 500 (^1H , 500 MHz; ^{13}C , 125 MHz) spectrometer and referenced to residual protio solvent.

Materials. Deuterated methylene chloride was dried over calcium hydride and vacuum distilled, followed by three freeze–pump–thaw cycles. Methyl oleate (>99%) was obtained from Nu-Chek-Prep (Elysian, MN) and stored over activated alumina. 1-Hexene was dried over calcium hydride, vacuum distilled, and freeze–pump–thawed prior to use. Allyl chloride (99%) was purchased from Aldrich and used as received.

Procedure for the Ethenolysis of Methyl Oleate. Ethenolysis reactions were carried out using research-grade methyl oleate (>99%) that was purified by storage over activated alumina followed by filtration. The experiments were set up in a glovebox under an atmosphere of argon. Methyl oleate was charged in a Fisher-Porter bottle equipped with a stir bar. A solution of ruthenium catalyst of an appropriate concentration was prepared in dry dichloromethane, and the desired volume of this solution was added to the methyl oleate. The head of the Fisher-Porter bottle was equipped with a pressure gauge, and a dip-tube was adapted on the bottle. The system was sealed and taken out of the glovebox to the ethylene line. The vessel was then purged with ethylene (polymer purity 99.9% from Matheson Tri Gas) for 5 min, pressurized to 150 psi, and placed in an oil bath at 40 °C. The reaction was monitored by collecting samples via the dip-tube at different reaction times. Prior to gas chromatography (GC) analysis, the reaction aliquots were quenched by adding a 1.0 M isopropanol solution of tris-hydroxymethylphosphine to each vial over the course of 2–3 h. The samples were then heated for over 1 h at 60 °C, diluted with distilled water, extracted with hexanes, and analyzed by GC. The GC analyses were run using a flame ionization detector. Column: Rtx-5 from Restek, 30 m \times 0.25 mm i.d. \times 0.25 μm film thickness. GC and column conditions: injection temperature, 250 °C; detector temperature, 280 °C; oven temperature, starting temperature, 100 °C; hold time, 1 min. The ramp rate was 10 °C/min to 250 °C, and the temperature was then held at 250 °C for 12 min. Carrier gas: helium.

Cross-Metathesis of 1-Hexene/Ethenolysis of 5-Decene Steady-State Experiments. In a glovebox under a nitrogen atmosphere, 0.5 mL of dry CD_2Cl_2 was added to an 8 in. NMR tube. 1-Hexene (18.9 μL , 0.149 mmol) was added via a 25 μL syringe, and the NMR tube was sealed with a septum cap. The appropriate amount of ruthenium catalyst (3 mol %) was added to a GC vial and dissolved in 0.25 mL of CD_2Cl_2 . The GC vial was capped and brought out of the glovebox along with the NMR tube. A ^1H NMR spectrum (Varian 500 MHz spectrometer) of the 1-hexene solution was taken for time point $t = 0$, and the catalyst solution was subsequently injected into the NMR tube via syringe through the septum cap. The septum cap was wrapped with parafilm, and the reaction progress was monitored over time by ^1H NMR spectroscopy. Catalyst stability was monitored by following the ruthenium benzylidene *H* peak over time, since catalyst decomposition causes the benzylidene *H* peak to shift or disappear altogether. Conversion of 1-hexene to 5-decene was determined by relative integration of the allylic CH_2 protons of 5-decene to those of 1-hexene. ^1H NMR of 1-hexene (CD_2Cl_2 , 500 MHz): δ 5.83 (ddt, $J = 17.0, 10.2, 6.7$ Hz, 1H), 5.02–4.96 (m, 1H), 4.92 (ddt, $J = 10.2, 2.3, 1.2$ Hz, 1H), 2.08–2.02 (m, 2H) [CH_2], 1.40–1.28 (m, 4H), 0.91 (t, $J = 5.0$ Hz, 3H) ppm. ^1H NMR of 5-decene (CD_2Cl_2 , 500 MHz): δ 5.43–5.38 (m, 1H), 2.00–1.91 (m, 2H) [CH_2], 1.34–1.28 (m, 4H), 0.90 (t, $J = 5.0$ Hz, 3H) ppm.

Cross-Metathesis of Allyl Chloride/Ethenolysis of 1,4-Dichloro-2-butene Steady-State Experiments. In a glovebox

under a nitrogen atmosphere, 0.5 mL of dry CD_2Cl_2 was added to an 8 in. NMR tube, and the NMR tube was sealed with a septum cap. The appropriate amount of ruthenium catalyst (3 mol %) was added to a GC vial and dissolved in 0.25 mL of CD_2Cl_2 . The GC vial was capped and brought out of the glovebox along with the NMR tube. Allyl chloride (12.2 μL , 0.150 mmol) was added via a 25 μL syringe through the septum cap, which was then wrapped with parafilm. ^1H NMR spectrum (Varian 500 MHz spectrometer) of the allyl chloride solution was taken for time point $t = 0$, and the catalyst solution was subsequently injected into the NMR tube via syringe through the septum cap. The reaction progress was monitored over time by ^1H NMR spectroscopy. Catalyst stability was monitored by following the ruthenium benzylidene H peak over time, since catalyst decomposition causes the benzylidene H to shift or disappear altogether. Conversion of allyl chloride to 1,4-dichloro-2-butene was determined by relative integration of the vinyl $\text{H}_2\text{C}=\text{CHCH}_2\text{Cl}$ proton of allyl chloride to the vinyl $\text{ClCH}_2\text{-CH}=\text{CHCH}_2\text{Cl}$ protons of 1,4-dichloro-2-butene. ^1H NMR of allyl chloride (CD_2Cl_2 , 500 MHz): δ 5.98 (ddt, $J = 10.0, 8.7, 6.6$ Hz, 1H), 5.35 (ddd, $J = 16.9, 2.5, 1.3$ Hz, 1H), 5.21 (ddd, $J = 10.1, 2.0, 0.9$ Hz, 1H), 4.09–4.05 (m, 2H) ppm. ^1H NMR of 1,4-dichloro-2-butene (CD_2Cl_2 , 500 MHz): δ 5.96–5.92 (m, 2H), 4.11–4.08 (m, 2H) ppm.

■ ASSOCIATED CONTENT

S Supporting Information. Experimental details for the synthesis of the catalysts and X-ray crystallographic data. This material is available free of charge via the Internet at <http://pubs.acs.org>.

■ AUTHOR INFORMATION

Corresponding Author
rhg@caltech.edu

■ ACKNOWLEDGMENT

This research was supported by the National Science Foundation through a Graduate Research Fellowship to R.M.T. B. K. K. acknowledges the NDSEG for a graduate fellowship. The authors acknowledge Drs. Lawrence Henling and Michael Day for obtaining the X-ray crystallographic structures of complexes **12** and **15**. We thank the NSF (CHE-1048404) and NIH (SR01GM031332-Z7) for funding and Materia, Inc. for the gift of methyl oleate and catalysts **1**, **2**, and **4**.

■ REFERENCES

- (1) (a) Grubbs, R. H. *Handbook of Metathesis*; Wiley-VCH: Weinheim, Germany, 2003 and references cited therein. (b) Cossy, J.; Arseniyadis, S.; Meyer, C. *Metathesis in Natural Product Synthesis*; Wiley-VCH: Weinheim, Germany, 2010.
- (2) Ritter, T.; Hejl, A.; Wenzel, A. G.; Funk, T. W.; Grubbs, R. H. *Organometallics* **2006**, *25*, 5740–5745.
- (3) (a) Fu, G. C.; Nguyen, S. T.; Grubbs, R. H. *J. Am. Chem. Soc.* **1993**, *115*, 9856–9857. (b) Chatterjee, A. K.; Morgan, J. P.; Scholl, M.; Grubbs, R. H. *J. Am. Chem. Soc.* **2000**, *122*, 3783–3784. (c) Trnka, T. M.; Grubbs, R. H. *Acc. Chem. Res.* **2001**, *34*, 18–29. (d) Love, J. A.; Morgan, J. P.; Trnka, T. M.; Grubbs, R. H. *Angew. Chem. Int. Ed.* **2002**, *41*, 4035–4037.
- (4) (a) Dias, E. L.; Nguyen, S. T.; Grubbs, R. H. *J. Am. Chem. Soc.* **1997**, *119*, 3887–3897. (b) Sanford, M. S.; Ullman, M.; Grubbs, R. H. *J. Am. Chem. Soc.* **2001**, *123*, 749–750. (c) Sanford, M. S.; Love, J. A.; Grubbs, R. H. *J. Am. Chem. Soc.* **2001**, *123*, 6543–6554.
- (5) (a) Chatterjee, A. K.; Choi, T. -L.; Sanders, D. P.; Grubbs, R. H. *J. Am. Chem. Soc.* **2003**, *125*, 11360–11370. (b) Ibrahim, I.; Yu, M.;

- Schrock, R. R.; Hoveyda, A. H. *J. Am. Chem. Soc.* **2009**, *131*, 3844–3845. (c) Malcolmson, S. J.; Meek, S. J.; Sattely, E. S.; Schrock, R. R.; Hoveyda, A. H. *Nature* **2008**, *456*, 933–937. (d) Jiang, A. J.; Zhao, Y.; Schrock, R. R.; Hoveyda, A. H. *J. Am. Chem. Soc.* **2009**, *131*, 16630–16631.
- (6) Anderson, D. R.; Ung, T.; Mkrtumyan, G.; Bertrand, G.; Grubbs, R. H.; Schrodi, Y. *Organometallics* **2008**, *27*, 563–566.
- (7) Burdett, K. A.; Harris, L. D.; Margl, P.; Maughon, B. R.; Mokhtar-Zadeh, T.; Saucier, P. C.; Wasserman, E. P. *Organometallics* **2004**, *23*, 2027–2047.
- (8) Mandelli, D.; Jannini, M. J. D. M.; Buffon, R.; Schuchardt, U. *J. Am. Oil Chem. Soc.* **1996**, *73*, 229–32.
- (9) Lysenko, Z.; Maughon, B. R.; Bicerano, J.; Burdett, K. A.; Christenson, C. P.; Cummins, C. H.; Dettloff, M. L.; Maher, J. M.; Schrock, A. K.; Thomas, P. J.; Varjian, R. D.; White, J. E. WO 2003/093215 A1, priority date of November 13, 2003.
- (10) (a) Olson, E. S. US 2010/0191008 A1, priority date of July 29, 2010. (b) DuBois, J.-L.; Sauvageot, O. WO 2010/103223 A1, priority date of September 16, 2010. (c) Herbinet, O.; Pitz, W. J.; Westbrook, C. K. *Combust. Flame* **2010**, *157*, 893–908.
- (11) (a) Mol, J. C. *J. Mol. Catal. A: Chem.* **2004**, *213*, 39–45. (b) Kuhn, K. M.; Bourg, J.-B.; Chung, C. K.; Virgil, S. C.; Grubbs, R. H. *J. Am. Chem. Soc.* **2009**, *131*, 5313–5320.
- (12) Marinescu, S. C.; Schrock, R. R.; Müller, P.; Hoveyda, A. H. *J. Am. Chem. Soc.* **2009**, *131*, 10840–10841.
- (13) Hong, S. H.; Wenzel, A. G.; Salguero, T. T.; Day, M. W.; Grubbs, R. H. *J. Am. Chem. Soc.* **2007**, *129*, 7961–7968.
- (14) (a) Patel, J.; Mujcinovic, S.; Jackson, W. R.; Robinson, A. J.; Serelis, A. K.; Such, C. *Green Chem.* **2006**, *8*, 450–454. (b) Bei, X.; Allen, D. P.; Pedersen, R. L. *Pharm. Technol.* **2008**, s18.
- (15) (a) Forman, G. S.; Bellabara, R. M.; Tooze, R. P.; Slawin, A. M. Z.; Karch, R.; Winde, R. *J. Organomet. Chem.* **2006**, *691*, 5513–5516. (b) Forman, G. S.; McConnell, A. E.; Hanton, M. J.; Slawin, A. M. Z.; Tooze, R. P.; van Rensburg, W. J.; Meyer, W. H.; Dwyer, C.; Kirk, M. M.; Serfontein, D. W. *Organometallics* **2004**, *23*, 4824–4827.
- (16) Schrodi, Y.; Ung, T.; Vargas, A.; Mkrtumyan, G.; Lee, C. W.; Champagne, T. M.; Pederson, R. L.; Hong, S. H. *Clean* **2008**, *36*, 669–673.
- (17) Stewart, I. C.; Keitz, B. K.; Kuhn, K. M.; Thomas, R. M.; Grubbs, R. H. *J. Am. Chem. Soc.* **2010**, *132*, 8534–8535.
- (18) Vehlou, K.; Maechling, S.; Blechert, S. *Organometallics* **2006**, *25*, 25–28.
- (19) Vehlou, K.; Wang, D.; Buchmeiser, M. R.; Blechert, S. *Angew. Chem. Int. Ed.* **2008**, *47*, 2615–2618.